Eur. Phys. J. A **15**, 399–404 (2002)
DOI 10.1140/epja/i2002-10043-7

THE EUROPEAN PHYSICAL JOURNAL A

Directed and elliptic flows in ^{40}Ca + ^{40}Ca and ^{112}Sn + ^{112}Sn collisions

H.Y. Zhang[1,a], W.Q. Shen[1,2], Y.G. Ma[1], X.Z. Cai[1], D.Q. Fang[1], L.P. Yu[1], C. Zhong[1], and Y.B. Wei[1]

[1] Shanghai Institute of Nuclear Research, Chinese Academy of Sciences, Shanghai 201800, PRC
[2] College of Sciences, Ningbo University, Ningbo 315211, PRC

Received: 15 March 2002 / Revised version: 11 June 2002 /
Published online: 19 November 2002 –
Communicated by W. Henning

Abstract. The directed and elliptic flows for different light particles and fragments in collisions of ^{40}Ca + ^{40}Ca and ^{112}Sn + ^{112}Sn at energies from 30 MeV/nucleon to 100 MeV/nucleon were studied in the isospin-dependent quantum molecule dynamics model (IQMD). With increasing incident energy, the directed flow rises from negative to positive, while the elliptic flow decreases with increasing the incident energies. The directed flow for the ^{40}Ca + ^{40}Ca system is not sensitive to the nuclear equation of states (EOS), but the directed flow for the ^{112}Sn + ^{112}Sn system is sensitive to the EOS. However, the elliptic flows for both ^{40}Ca + ^{40}Ca and ^{112}Sn + ^{112}Sn systems are not sensitive to EOS. A study of the dependence of directed and elliptic flows on the fragment charge (mass) is also performed.

PACS. 25.75.-q Relativistic heavy-ion collisions – 24.10.Lx Monte Carlo simulations (including hadron and parton cascades and string breaking models) – 25.70.-z Low and intermediate energy heavy-ion reactions

1 Introduction

Heavy-ion collisions (HIC) at intermediate and high energies provide a possibility of studying the properties of nuclear matter at different temperatures and different densities. The nuclear equation of state (EOS) can be researched via liquid-gas transition, multi-fragmentation and collective flow produced in heavy-ion collisions [1–3]. Its knowledge is not only of interest in nuclear physics but is also useful in understanding astrophysical phenomena such as the evolution of the early universe and the scenario of supernova explosions. One observable that has been extensively used for extracting EOS from heavy-ion collisions is the collective flow of various particles [4, 5]. The collective flow for different fragments deflected sideward from the hot and dense region formed by the overlap of projectile and target nuclei [6,7] was called transverse flow or directed flow and this was often used to extract the EOS. Such preferential emission of a particle or a fragment is considered an important signature of nuclear compression and expansion. In recent years, much emphasis has been put on the study of the collective flow and several groups have already performed experiments to study its disappearance [8–13] at a balance energy which is closely related to the EOS. Experiments indicated an energy dependence of the flow which changes from negative to positive with increasing the incident energy and indicated a dominant interaction between two colliding nuclei from mean-field interaction to nucleon-nucleon collisions. The dependence of the directed flow on the fragment mass was observed also for charge $Z = 1$ and $Z = 2$ particles at energies up to 0.4 AGeV [14–16]. This observation suggests that heavier fragments may carry more direct information on the bulk properties of nuclear matter. But a systematic understanding of the mass dependence of the collective fragment flow is lacking. So it is important to study the fragment formation, the directed flow and the elliptic flow because it would provide valuable data on the nuclear EOS and isospin-dependent N-N cross-sections. In particular, the excitation function of the transverse collective flow from low to ultra-relativistic energies has been found especially interesting. On the high-energy side, a minimum of the collective flow is expected in reactions crossing the phase transition region from hadronic matter to Quark-Gluon-Plasma. At intermediate energies, the transverse collective flow disappears at an incident energy, termed balance energy $E_{\rm bal}$. This phenomenon has been well established by many experiments during the last decade. Simultaneously, much theoretical work has been devoted to understand the mechanism responsible for the disappearance of

[a] e-mail: Zhanghy@sinr.ac.cn;
Permanent address: Shanghai Institute of Nuclear Research, Chinese Academy of Sciences, P.O. Box 800-204(2), Shanghai 201800, China.

the transverse flow at the balance energy. It has long been suggested that at balance energies the attractive scattering dominant at energies around 10 MeV/nucleon balances the repulsive interactions dominant at energies around 400 MeV/nucleon. These efforts, however, have been severely hindered by the dual sensitivities of balance energies to both the nuclear EOS and the in-medium nucleon-nucleon cross-sections [17,18]. The influence of in-medium nucleon-nucleon cross-sections had been investigated by measuring the experimental reaction cross-sections [19]. From ref. [19], $0.8\sigma_{\rm cug}$ is much better than $0.6\sigma_{\rm cug}$ and $\sigma_{\rm cug}$ by fitting experimental reaction cross-sections. So, we adopt the in-medium cross-sections $0.8\sigma_{\rm cug}$ in the IQMD for the calculation of the directed and elliptic flows.

Recently, the isospin dependence of the collective flow has also become an interesting subject of theoretical and experimental investigation [20,21]. One knows that the nuclear collective flow is a kind of collective phenomenon found in intermediate- and high-energies heavy-ion collisions, and the studies of the dependence of the directed flow, the elliptic flow and the different-fragments flow on beam energies, mass number, isospin and impact parameter have revealed much interesting physics about the properties and origin of the collective flow. In past years, either the directed flow or the elliptic flow has been studied separately in some papers, but combined researches with consideration of isospin dependence are still very few. In this paper, an endeavor will be made in this direction with the isospin-dependent quantum molecule dynamics method.

2 QMD and IQMD model

The isospin dependence of collective flow has been studied by Li *et al.* [22] and Zheng *et al.* [23] in terms of an isospin-dependent Boltzmann-Uehling-Uhlenbeck (IBUU) model in which the initial proton and neutron densities were calculated from the nonlinear relativistic mean-field (RMF) theory while the isospin dependence enters into the model by using the isospin-dependent nuclear mean field. The IBUU treats protons and neutrons explicitly and includes an asymmetry term in the nuclear mean-field potential and different scattering cross-section for protons and neutrons. However , the IBUU model cannot describe the flow for different fragments well since it is a one-body transport model and does not contain many-body correlation.

In the quantum molecule dynamics (QMD) model, nuclei are represented by Gaussian-shaped density distributions. They are initialized in a shape with radius $R = 1.12A^{1/3}$, according to the liquid-drop model. Each nucleon is supposed to occupy a volume $\hbar^3$, so that the phase space is uniformly filled. The QMD model is a n-body theory which simulates heavy-ion reactions at intermediate energies on an event-by-event basis.

In order to explain experimental results much better, the original version of the QMD model [24] was improved to include isospin degrees of freedom explicitly and include the isospin dependence as for the Coulomb potential, symmetry potential, N-N cross-sections and Pauli blocking, and this was called the IQMD model. The former IQMD model [25] only includes the isospin dependence as for a symmetry potential and explicit Coulomb forces between the $Z_{\rm P}$ and $Z_{\rm T}$ protons. In addition, in initialization of projectile and target nuclei via using the nonlinear relativistic mean-field (RMF) theory [26], neutrons and protons will be sampled in phase space separately because of the great difference between proton and neutron density distributions for nuclei far from the β-stability line. The coordinates of the particle ground state and momentum distribution can be achieved by analyzing the time evolution. Some isospin effects of heavy-ion collisions at intermediate energies can be successfully explained with the IQMD model [27,28]. Using the IQMD model, we have studied the directed and elliptic flows and the flow of different fragments in the reactions of the ^{112}Sn + ^{112}Sn and ^{40}Ca + ^{40}Ca systems which have a great difference in the combined mass. Meanwhile, the roles of the impact parameter and the nuclear EOS have also been studied in this paper.

The IQMD model can explicitly represent the many-body state of the system and contains correlation effects to all orders and all fluctuations. It has basically two advantages: 1) the many-body process, in particular, the formation of complex fragments is treated and 2) the model allows for an event-by-event analysis of heavy-ion reactions similar to the methods which is used for the analysis of experimental high-acceptance data. The IQMD model provides some information about both the collision dynamics and the fragmentation process. Even though the BUU model can describe the one-body observable very successfully, it cannot describe the formation of the cluster well. In this work, the fragment is recognized in terms of the so-called modified coalescence model, in which particles with a relative momentum smaller than P_0 and a relative distance smaller than R_0 are considered to belong to one fragment. We adopted the parameters $R_0 = 2.4$ fm and $P_0 = 200$ fm/c. Then we checked further whether the fragment is or is not an isotope existing in the nuclear data sheets. If it is, the fragment can be accepted. Meanwhile, in order to get rid of the nonphysical fragments, only the reasonable fragments are selected. Therefore, the present model to construct fragments is an extended version of the conventional coalescence model by considering self-consistently the isospin constraint and aggregation procedure.

The time evolution of the system is determined by the classical canonical equation of motion

$$\dot{p}_i = -\frac{\partial\langle H\rangle}{\partial r_i}; \qquad \dot{r}_i = \frac{\partial\langle H\rangle}{\partial P_i}. \tag{1}$$

The IQMD model is classical in essence as shown in eq. (1). However, many important quantum features are included in the model. A comprehensive review can be found in ref. [21].

3 Calculation and results

Taking the beam direction along the Z-axis and the reaction plane on the X-Z plane, the elliptic flow is then de-

termined from the average difference between the square of the X and Y components of the particles transverse momentum [29–32], *i.e.*

$$V_2 = \left\langle \frac{P_x^2 - P_y^2}{P_x^2 + P_y^2} \right\rangle. \quad (2)$$

It corresponds to the second Fourier coefficient in the transverse-momentum distribution [33,34]. $V_2 > 0$ describes the eccentricity of an ellipse-like distribution and indicates the in-plane enhancement of particle emission, a rotational behavior. While $V_2 < 0$ shows the property of the squeeze-out effect perpendicular to the reaction plane. $V_2 = 0$ means the isotropic distribution in the transverse plane. Usually, $V_2 = 0$ is extracted from the mid-rapidity region. The directed-flow parameter at mid-rapidity is defined by

$$F = \left. \frac{\mathrm{d}\langle P_x \rangle}{\mathrm{d}y} \right|_{y_{\mathrm{cm}}=0}. \quad (3)$$

The potential of the IQMD model used in the present study includes an asymmetry term in the nuclear mean-field potential. The nuclear mean-field potential is parameterized as

$$U(\rho, \tau_z) = \alpha\left(\frac{\rho}{\rho_0}\right) + \beta\left(\frac{\rho}{\rho_0}\right)^{\sigma} + c\left(\frac{\rho_p - \rho_n}{\rho_0}\right)\tau_z, \quad (4)$$

where ρ_0 is the normal nuclear density; ρ, ρ_n and ρ_p are the nucleon, neutron and proton densities, respectively; and τ_z equals 1 for protons and -1 for neutrons and c is chosen to be 32 MeV. The total interaction potential of the system in the IQMD model is given by

$$U^{\mathrm{tot}} = U + U^{\mathrm{Yuk}} + U^{\mathrm{Coul}} + U^{\mathrm{Sym}} + U^{\mathrm{MDI}} \quad (5)$$

with U the density-dependent potential, U^{Yuk} the Yukawa potential, U^{Coul} the Coulomb energy, U^{Sym} the symmetry energy term, and the U^{MDI} momentum-dependent interaction. We have chosen a stiff equation of state with a compressibility of $K = 380$ MeV or a soft equation of state with a compressibility of $K = 220$ MeV.

The directed and elliptic flows and the flow of the fragment in the reactions ^{40}Ca + ^{40}Ca and ^{112}Sn + ^{112}Sn are calculated at different incident energies, different impact parameters and different EOSs. The directed flow is related to the slope of the in-plane transverse momentum on the mid-rapidity ($|y/y_p| \leq 0.25$) in the c.m. system. For each impact parameter, a calculation of 1000 events is performed. In the present calculations, it is found that the directed and elliptic flows have been saturated around a time of 120 fm/c. The results shown here actually correspond to the statistical average value of 5000 "events" which come from the sum of five time intervals from 120 to 200 fm/c in each event.

As we know, the symmetry energy is very important in the nuclear potential for asymmetrical nuclear matter. In this work, the symmetry energy c is chosen to be 32 MeV. From fig. 1(a), we can clearly see that the density distribution of the proton and neutron is almost the same in the ^{40}Ca nucleus. But there still is a little difference between the proton and neutron density when the distance is large enough. The symmetry energy plays just a little role for the nuclear potential of such nuclei. The elliptic and directed flows are almost the same for different symmetry energies [35]. But for ^{112}Sn, the density distribution of the proton and neutron has a greater difference than for the case of the ^{40}Ca nucleus, the symmetry energy may play a more important role for the nuclear potential. The elliptic and directed flows may have a big difference for different symmetry energies due to greatly different proton and neutron density distributions in ^{112}Sn, see fig. 1(b). It seems that the symmetry energy is sensitive to those nuclei which have a large proton-neutron ratio. The density distributions of proton, neutron and matter for ^{40}Ca and ^{112}Sn in fig. 1 are calculated by using the Relativistic Mean-field (RMF) theory. The solid line corresponds to the matter distribution, the dotted line to the proton distribution and the dashed line to the neutron distribution in ^{40}Ca and ^{112}Sn nuclei.

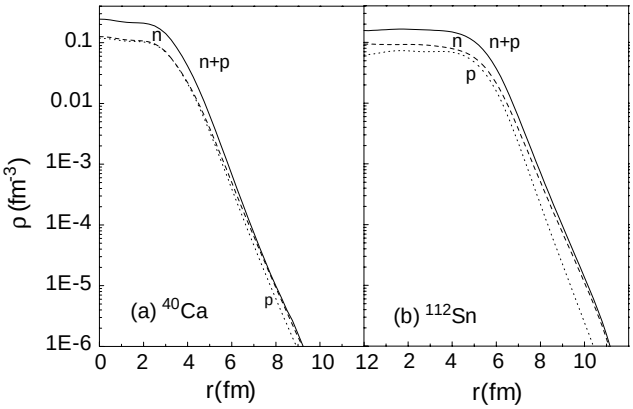

Fig. 1. Density distribution of proton (dotted line), neutron (dashed line) and matter (solid line) for ^{40}Ca + ^{40}Ca collisions (a) and ^{112}Sn + ^{112}Sn collisions (b) by using the Relativistic Mean-field (RMF) theory.

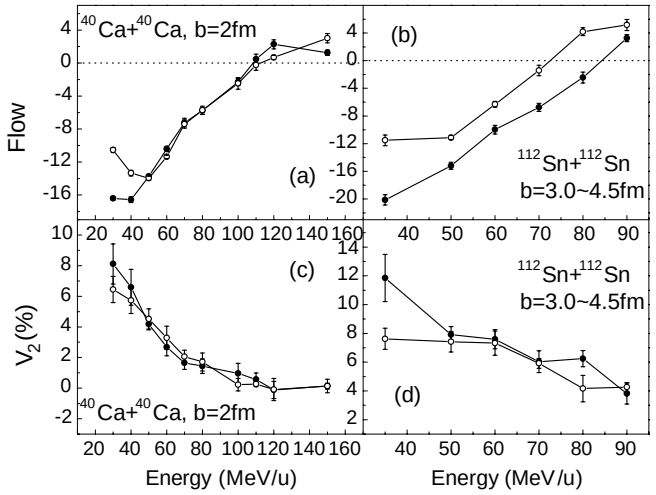

Fig. 2. Directed and elliptic flows of all particles for ^{40}Ca + ^{40}Ca and ^{112}Sn + ^{112}Sn collisions at different incident energies, • for soft EOS and ∘ for stiff EOS.

Figure 2 shows the directed flow and elliptic flow for ^{40}Ca + ^{40}Ca and ^{112}Sn + ^{112}Sn collisions at different incident energies. Solid-dot symbols correspond to soft potential and open-dot symbols to stiff potential. From fig. 2(a) and (b), we see that the directed flow increases with increasing incident energy. For the ^{40}Ca + ^{40}Ca system, the balance energy, *i.e.*, the energy of disappearance of the directed flow is almost the same near 110 MeV for soft and stiff EOSs, see fig. 2(a). But the balance energy of the ^{112}Sn + ^{112}Sn system is different for soft and stiff EOSs. With the soft potential it is near 85 MeV and with the stiff potential it is near 70 MeV, see fig. 2(b). The balance energy of the directed flow for the soft potential is larger than that of the stiff potential for ^{112}Sn + ^{112}Sn. From the comparison of the two systems, the directed flow of the ^{112}Sn + ^{112}Sn system is sensitive to the equation of nuclear state (EOS) and that of ^{40}Ca + ^{40}Ca is not very sensitive to the EOS. It probably implies that the different system mass includes the different sensitivity to the EOS as pointed out in ref. [16]. In ref. [16], the mass dependence of the disappearance of the directed flow in nuclear collisions was shown. However, when the system mass is around 70, the balance energy is not sensitive to the EOS. However, when the system mass is large or small enough, the difference of balance energy is shown for the soft EOS and the stiff EOS. ^{40}Ca and ^{112}Sn differ not only in isospin but also in mass. A system size dependence of the balance energy has been observed experimentally. The sensitivity of the balance energy to the EOS in ^{112}Sn + ^{112}Sn might be the increased stopping in the heavier system. This effect can be studied by switching off the isospin-dependent parameters in the IQMD model. The Boltzmann-Uehling-Uehlenbeck (BUU) model was used in ref. [16]. Compared with the experimental balance energy, BUU calculations can reproduce the scaling with mass but underestimate the balance energy $E_{\rm bal}$ systematically. The IQMD fits the incident-energy dependence of the directed flow and also the scaling with mass of the balance energy, but the value of $E_{\rm bal}$ in IQMD is in general larger than the experimentally measured value [36,37]. Our calculations agree with this. In fig. 2(c) and (d), all the values of the elliptic flow are positive and decrease with increasing the incident energy which indicates that the rotational behavior becomes weak with increasing the incident energy, but the squeeze-out never reveals below 90 MeV/nucleon for both systems, even though the directed flow changes from negative to positive. For ^{40}Ca + ^{40}Ca and ^{112}Sn + ^{112}Sn at 30 MeV/nucleon the incident energy is smaller, the elliptic flow is greatly different in the case of the soft potential with respect to the case of the stiff potential due to the fact that the N-N scattering effect at low energies is not strong enough and the nuclear mean-field potential is dominant. However, there will be only a small difference in the elliptic flow between the soft potential and the stiff potential with larger incident energy. Overall, the elliptic flow is not very sensible to the nuclear EOS in the studied reaction systems. The quoted error bars in the figure are statistical errors.

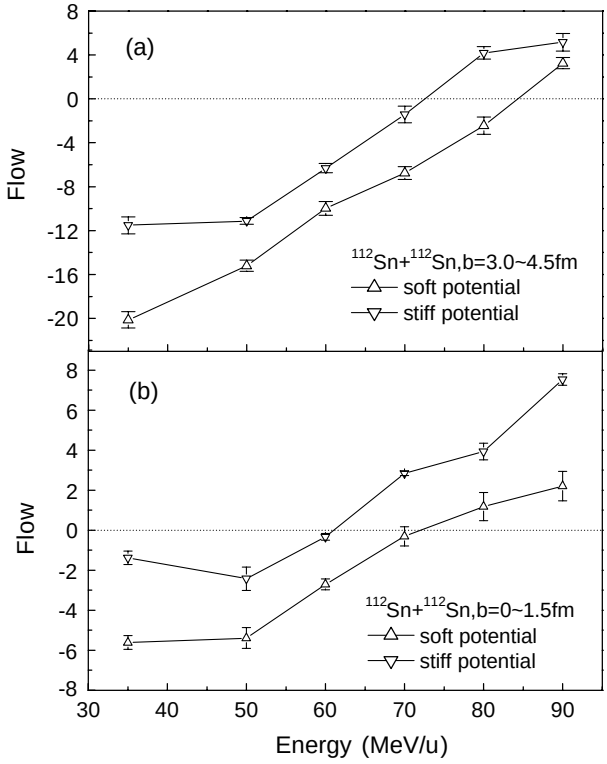

Fig. 3. Directed flows of all particles for ^{112}Sn + ^{112}Sn collisions at different impact parameters, △ for soft EOS and ▽ for stiff EOS.

In order to study systematically the relationship of the balance energy with the impact parameter and the interaction potential, the ^{112}Sn + ^{112}Sn system is carefully investigated at different impact parameters with different potentials. When the impact parameter is 3.0–4.5 fm, the balance energy with the soft potential is near 85 MeV and that with the stiff potential is near 70 MeV as shown in fig. 3(a). While the impact parameter is 0–1.5 fm, the balance energy with the soft potential is near 70 MeV and that with the stiff potential is near 60 MeV, as shown in fig. 3(b). In fig. 3, the up-triangles correspond to the soft potential and the down-triangles to the stiff potential. Therefore, the balance energy depends strongly on the nuclear equation of state as well as the impact parameter for ^{112}Sn + ^{112}Sn. In ref. [38,39], the balance energy has been measured for a large range of systems. Central collisions are adopted in an experiment which is almost in agreement with our calculation. If one wanted to extract some information on the nuclear equation of state from the excitation function of the directed flow for a system like ^{112}Sn + ^{112}Sn, the effect of the impact parameter on the directed flow should be considered carefully.

The investigation of the directed and elliptic flows at different impact parameters are made and compared in fig. 4. Figure 4 shows the impact parameter dependence of directed and elliptic flows. The four impact parameter regions 0–1.5 fm, 1.5–3.0 fm, 3.0–4.5 fm, 4.5–6.0 fm for the ^{112}Sn + ^{112}Sn system and the four impact parameters 0 fm, 2 fm, 3.8 fm and 6 fm for the ^{40}Ca + ^{40}Ca system

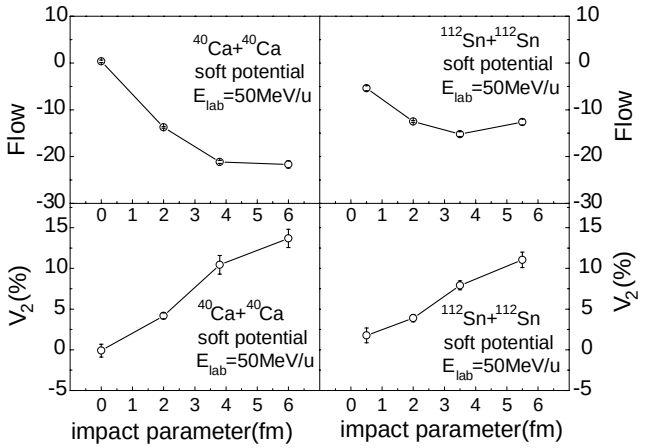

Fig. 4. Directed and elliptic flows of all particles for ^{40}Ca + ^{40}Ca (left) and ^{112}Sn + ^{112}Sn (right) collisions for different impact parameters at an incident energy of 50 MeV/nucleon.

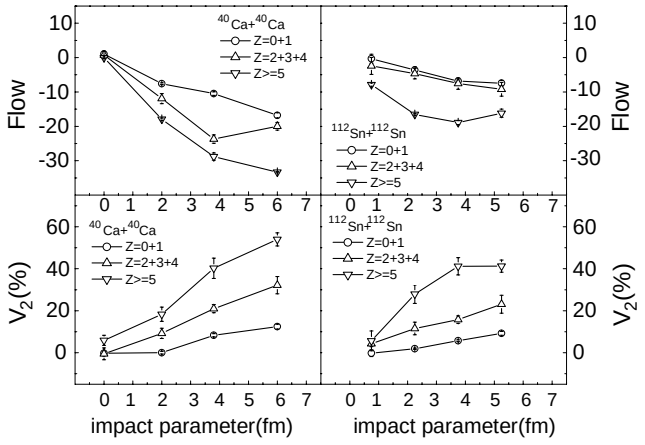

Fig. 6. Dependence of directed and elliptic flows of different fragments on impact parameters for ^{40}Ca + ^{40}Ca (left) and ^{112}Sn + ^{112}Sn (right).

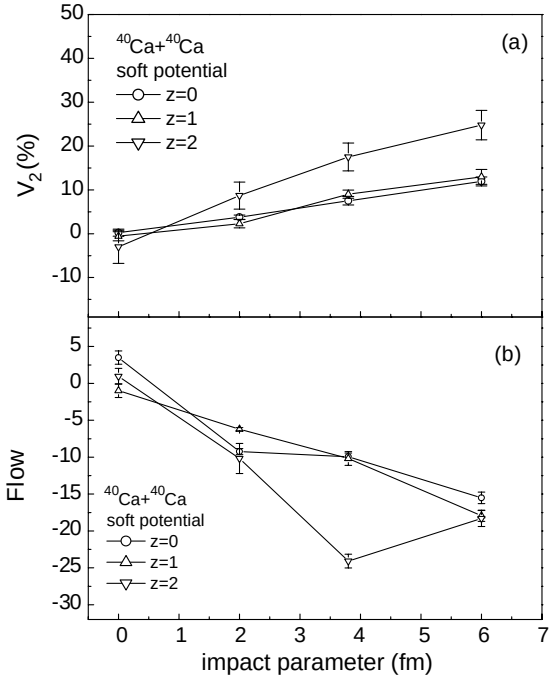

Fig. 5. Dependence of directed and elliptic flows of different fragments for ^{40}Ca + ^{40}Ca on different impact parameters with soft EOS.

at an incident energy of 50 MeV/nucleon are used in the calculation. The directed flows are all negative while the elliptic flows are all positive at different impact parameters for both systems at this energy. The directed and elliptic flows strongly depend on the impact parameters. When the impact parameter increases, the absolute value of the directed flow increases and reaches saturation approximately in semi-peripheral collisions, while the elliptic flow increases in the positive direction. These observations are consistent with the experimental observation and other theoretical works [40–45].

As mentioned above, one advantage of the IQMD model is its fragment formation. In addition, some important dynamics and the process of disintegration information can be achieved. According to the charge number, we extract three kinds of different fragment flows. The open circles represent the flow of fragments with $Z = 0$; the open up-triangles represent the flow of fragments with $Z = 1$ and the open down-triangles represent the flow of fragments with $Z = 2$. At an incident energy of 50 MeV/nucleon and the four impact parameters, *i.e.* 0 fm, 2 fm, 3.8 fm and 6 fm for the ^{40}Ca + ^{40}Ca system, fig. 5 shows that the absolute values of the directed and the elliptic flows enhance as the charge number increases. Because of the low statistical number, there is statistical fluctuation. In order to accumulate the sufficient statistics and reduce the statistical fluctuation, we define three bins of different fragment regions according to the charge number: the open circles represent the flow of the fragment of neutrons and $Z = 1$ particles; the open up-triangles represent the flow of fragments with $Z = 2$–4 and the open down-triangles represent the flow of fragments with $Z \geq 5$. At an incident energy of 50 MeV/nucleon for the ^{40}Ca + ^{40}Ca and ^{112}Sn + ^{112}Sn systems with the same impact parameter as above, the absolute values of the directed and the elliptic flows enhance as the charge (or mass) increases, *i.e.* the heavier fragment flow is stronger than the light one, see fig. 6 with better statistics.

In order to further investigate the elliptic flow of different fragments, the excitation function of the elliptic flow of different fragments for ^{40}Ca + ^{40}Ca at $b = 2$ fm with the stiff potential and the soft potential is depicted in fig. 7. From fig. 7, the elliptic flows of heavier fragments are much larger than those of lighter fragments with either the soft or the stiff potential. The elliptic flow decreases with increasing incident energies. There is an obvious difference among the three different fragments at low incident energy. When the incident energy increases, the difference between the elliptic flow of the different fragments decreases. Around 100 MeV/nucleon the elliptic flow changes very slowly with incident energy and tends to vanish. But the squeeze-out which has a negative elliptic flow never happens below incident energies

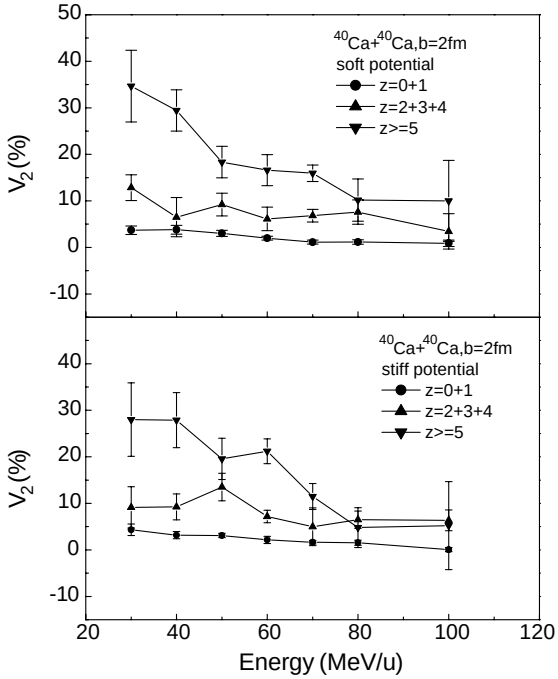

Fig. 7. Dependence of the elliptic flow on incident energy for different fragments with stiff and soft potentials.

less than 100 MeV/nucleon. Maybe, the squeeze-out will happen even at high energies for these two systems. From these calculations it is shown that the elliptic flow is not very much sensitive to the potential for these two systems at incident energies below 100 MeV/nucleon.

4 Summary and conclusions

In summary, the IQMD model has been used to study the directed and elliptic flows in the collisions of ^{40}Ca + ^{40}Ca and ^{112}Sn + ^{112}Sn at different impact parameters and different fragment flows from 30 to 100 MeV/nucleon. It is found that a transition in the directed flow from negative to positive is revealed as the incident energy increases. A strong dependence on the nuclear EOS is seen in the directed flow at different incident energies for ^{112}Sn + ^{112}Sn, but this is not so for ^{40}Ca + ^{40}Ca. For both systems the directed flow depends strongly on the impact parameters. The elliptic flow decreases with increasing incident energy and increases with increasing impact parameter for both systems. The elliptic flow and the directed flow are observed to be stronger as the fragment charge/mass increases for both systems. In comparison with the directed flow, the elliptic flow is not very sensitive to the EOS for both systems. By this study, we find that there may exist a different sensitivity to EOS for different kind of flow and different systems. Hence, it will be helpful to choose the system and type of flow for probing the EOS before the comparison with the data is made.

This work was supported by the Major State Basic Research Development Program under Contract No. G200077400, National Natural Sciences Funds for Distinguished Young Scholar (19725521) and National Natural Sciences Foundation of China (19705012).

References

1. G. Peilert *et al.*, Rep. Prog. Phys. **57**, 533 (1994).
2. L.G. Moretto, G.J. Wozniak, Annu. Rev. Nucl. Part. Sci. **43**, 379 (1993).
3. J. Pochodzalla *et al.*, Phys. Rev. Lett. **75**, 1040 (1995).
4. P. Danielewicz *et al.*, Phys. Lett. B **157**, 146 (1985).
5. W. Scheid *et al.*, Phys. Rev. Lett. **32**, 741 (1974).
6. H.H. Gutbrod, A.M. Poskanzer, H.G. Ritter, Rep. Prog. Phys. **52**, 1267 (1989).
7. H. Stöcker, W. Greiner, Phys. Rep. **57**, 559 (1986).
8. C.A. Ogilvie *et al.*, Phys. Rev. C **42**, R101 (1990).
9. D. Krofcheck *et al.*, Phys. Rev. Lett. **63**, 2028 (1989).
10. J.P. Sullivan *et al.*, Phys. Lett. B **249**, 8 (1990).
11. W.M. Zhang *et al.*, Phys. Rev. C **42**, R491 (1990).
12. D. Krofcheck *et al.*, Phys. Rev. C **43**, 350 (1991).
13. D. Krofcheck *et al.*, Phys. Rev. C **46**, 1416 (1992).
14. M.B. Tsang *et al.*, Phys. Rev. Lett. **57**, 559 (1986).
15. K.G.R. Doss *et al.*, Phys. Rev. Lett. **59**, 2720 (1987).
16. G.D. Westfall *et al.*, Phys. Rev. Lett. **71**, 1986 (1993).
17. J. Molitoris, H. Stöcker, Phys. Lett. B **162**, 47 (1998).
18. G.F. Bertsch, W.G. Lynch, M.B. Tsang, Phys. Lett. B **189**, 738 (1987).
19. Y.G. Ma, W.Q. Shen, Phys. Rev. C **48**, 850 (1993).
20. R. Pak *et al.*, Phys. Rev. Lett. **78**, 1022 (1997).
21. R. Pak *et al.*, Phys. Rev. Lett. **78**, 1026 (1997).
22. B.A. Li, Z.Z. Ren, C.M. Ko, S.J. Yennello, Phys. Rev. Lett. **76**, 4492 (1996); B.A. Li, Phys. Rev. Lett. **85**, 4221 (2000).
23. Y.M. Zheng *et al.*, Phys. Rev. Lett. **83**, 2534 (1999).
24. J. Aichelin, Phys. Rep. **202**, 233 (1991).
25. S.A. Bass, C. Hartnack, H. Stöcker, W. Greiner, Phys. Rev. C **51**, 3343 (1995).
26. Z.Y. Zhu, W.Q. Shen, Y.H. Cai, Y.G. Ma, Phys. Lett. B **328**, 1 (1994).
27. L.W. Chen, X.D. Zhang, L.X. Ge, High En. Phys. Nucl. Phys. **20**, 1091 (1998) (in Chinese).
28. B. Chen, J.Y. Liu, F.S. Zhang *et al.*, High En. Phys. Nucl. Phys. **24**, 244 (2000) (in Chinese).
29. J. Appelshauser *et al.*, Phys. Rev. Lett. **80**, 4136 (1998).
30. P. Danielewicz *et al.*, Phys. Rev. Lett. **81**, 2438 (1998).
31. Y. Shin *et al.*, Phys. Rev. Lett. **81**, 1576 (1998).
32. H. Sorge *et al.*, Phys. Rev. Lett. **82**, 2048 (1999).
33. S.A. Voloshin *et al.*, Phys. Rev. C **55**, R1630 (1997); A.M. Poskanzer, S.A. Voloshin, Phys. Rev. C **58**, 1671 (1998).
34. A.M. Poskanzer *et al.*, Phys. Rev. C **58**, 1671 (1998).
35. H.Y. Zhang, Y.G. Ma, L.P. Yu, *et al.*, High En. Phys. Nucl. Phys. **25**, 1184 (2001) (in Chinese).
36. S. Soff *et al.*, Phys. Rev. C **51**, 3320 (1995).
37. R.J. Snelling, PhD Thesis, Utrecht University, 1998, ISBN 90-393-1634-1.
38. A. Buta *et al.*, Nucl. Phys. A **584**, 397 (1995).
39. G.D. Westfall, Nucl. Phys. A **630**, 27c (1998).
40. J. Péter *et al.*, Nucl. Phys. A **598**, 611 (1995).
41. Z.Y. He *et al.*, Nucl. Phys. A **598**, 248 (1996).
42. W.Q. Shen *et al.*, Nucl. Phys. A **551**, 333 (1993).
43. Y.G. Ma *et al.*, Z. Phys. A **346**, 285 (1993).
44. Y.G. Ma *et al.*, Phys. Rev. C **51**, 1029 (1995).
45. Y.G. Ma *et al.*, Phys. Rev. C **51**, 3256 (1995).